# REPORT No. 908

## STABILITY DERIVATIVES OF TRIANGULAR WINGS AT SUPERSONIC SPEEDS

By HERBERT S. RIBNER and FRANK S. MALVESTUTO, Jr.


### SUMMARY

*The analysis of the stability derivatives of low-aspect-ratio triangular wings at subsonic and supersonic speeds, given in NACA TN No. 1423, is extended to apply to triangular wings having large vertex angles and traveling at supersonic speeds. The lift, rolling moment due to sideslip, and damping in roll and pitch for this more general case have been treated elsewhere on the basis of the theory of small disturbances. The surface potentials for angle of attack and rolling taken therefrom are used to obtain the several side-force and yawing-moment derivatives that depend on leading-edge suction, and a tentative value for the rolling moment due to yawing. The lift and moment due to downward acceleration are obtained on the basis of an unpublished unsteady-flow solution. All the known stability derivatives of the triangular wing at supersonic speeds, regardless of source, are summarized for convenience and presented with respect to both body axes and stability axes. The results are limited to Mach numbers for which the triangular wing is contained within the Mach cone from its vertex. The spanwise variation of Mach number in the case of yawing is neglected, although the effect must be of importance.*


### INTRODUCTION

An earlier investigation (reference 1) has provided theoretical stability derivatives of low-aspect-ratio wings of triangular plan form at subsonic and supersonic speeds. The restriction to low aspect ratio was a consequence of the limitations of the theory. Several investigators have since obtained pressure distributions for angle of attack, rolling, pitching, and sideslip at supersonic speeds (references 2 to 6 and unpublished analyses), without restriction to low aspect ratio. These derivations have employed variants of the linear theory of supersonic flow and have, in fact, constituted important steps in the development of the theory.

If the rotations are taken about the vertex, the pressure distribution for each motion in the more general case is found to have the same shape as the corresponding low-aspect-ratio approximation, so long as the triangular wing is contained within the Mach cone from the vertex. The magnitudes differ by factors which are functions solely of the ratio of the tangent of the semivertex angle of the triangle to the tangent of the Mach angle. The same similarity exists between the distributions of surface potential. It is thus relatively simple to extend most of the derivations of reference 1 to remove the restriction of low aspect ratio for supersonic speeds. Such an extension is made in the present report.

The lift-curve slope, the damping in roll and pitch, and (in effect) the rolling moment due to sideslip have been evaluated in references 2 to 6, so that the principal contributions of the present report are the normal acceleration derivatives obtained on the basis of an unpublished unsteady-flow solution due to Clifford S. Gardner, the several side-force and yawing-moment derivatives, and a tentative value of the rolling moment due to yawing. All the known stability derivatives of the triangular wing at supersonic speeds, regardless of source, are collected herein for convenience and presented with respect to both body axes and stability axes. Wings with dihedral are not treated (although they were included in reference 1), and the results are limited to Mach numbers for which the wing is contained within the Mach cone from its vertex.

### SYMBOLS

| | |
|---|---|
| $x, y, z$ | rectangular coordinates (fig. 1) |
| $t$ | time |
| $u, v, w$ | incremental flight velocities along $x$-, $y$-, and $z$-axes, respectively (fig. 2); induced flow velocities along $x$-, $y$-, and $z$-axes of figure 1, respectively |
| $p, q, r$ | angular velocities about $x$-, $y$-, and $z$-axes, respectively (fig. 2) |

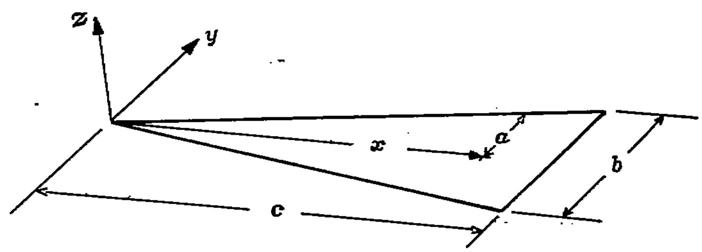


FIGURE 1.—Axes and notation used in analysis.

| | |
|---|---|
| $V$ | flight speed |
| $\bar{a}$ | speed of sound in free stream |
| $M$ | stream Mach number $(V/\bar{a})$ |
| $M'$ | component of the Mach number normal to wing leading edge $\left(\frac{MC}{\sqrt{1+C^2}}\right)$ |
| $B$ | cotangent of Mach angle $(\sqrt{M^2-1})$ |
| $\alpha$ | angle of attack (Flight $w/V$) |
| $\beta$ | angle of sideslip (Flight $v/V$) |
| $\epsilon$ | semivertex angle of triangle |
| $\mu$ | Mach angle $(\cot^{-1}\sqrt{M^2-1})$ |
| $\Delta P$ | local pressure difference between lower and upper surfaces of airfoil, positive in sense of a lift |
| $\rho$ | density of air |
| $a$ | semiwidth of triangle at distance $x$ from vertex |
| $b$ | span (base of triangle) |

$c$ root chord (height of triangle)

$\bar{c}$ mean aerodynamic chord
$\left(\bar{c}\equiv\frac{2}{S}\int_0^{b/2}(\text{Local chord})^2 dy=\frac{2}{3}c\right)$

$C$ edge slope $\left(\frac{a}{x}=\frac{da}{dx}=\frac{A}{4}=\frac{b}{2c}\right)$

$A$ aspect ratio $(2b/c)$

$S$ area of triangle $\left(\frac{1}{2}bc\right)$

$\phi$ velocity potential

$\psi$ value of $\phi$ for unit pitching velocity about $y$-axis

$\chi$ value of $\phi$ for unit angle of attack

$\eta=\cos^{-1}\frac{y}{a}$

$k=\sqrt{1-B^2C^2}$

$E'(BC)$ complete elliptic integral of the second kind with modulus $k$ $\left(\int_0^{\frac{\pi}{2}}\sqrt{1-k^2\sin^2 z}\,dz\right)$

$F'(BC)$ complete elliptic integral of the first kind with modulus $k$ $\left(\int_0^{\frac{\pi}{2}}\frac{dz}{\sqrt{1-k^2\sin^2 z}}\right)$

$E''(BC)=\frac{1}{E'(BC)}$

$Q(BC)=\frac{[E''(BC)]^2}{\sqrt{1-B^2C^2}}$

$G(BC)=\frac{1-B^2C^2}{(1-2B^2C^2)E'(BC)+B^2C^2F'(BC)}$

$H(BC)=3G(BC)-2E''(BC)$

$I(BC)=\frac{2(1-B^2C^2)}{(2-B^2C^2)E'(BC)-B^2C^2F'(BC)}$

$J(BC)=E''(BC)I(BC)\sqrt{1-B^2C^2}$

$K$ constant defined in equation (16)

$N$ yawing moment

$Y$ lateral force

$f$ suction force per unit length of edge

$C_L$ lift coefficient $\left(\frac{\text{Lift}}{\frac{1}{2}\rho V^2 S}\right)$

$C_m$ pitching-moment coefficient $\left(\frac{\text{Pitching moment}}{\frac{1}{2}\rho V^2 S\bar{c}}\right)$

$C_l$ rolling-moment coefficient $\left(\frac{\text{Rolling moment}}{\frac{1}{2}\rho V^2 Sb}\right)$

$C_n$ yawning-moment coefficient $\left(\frac{N}{\frac{1}{2}\rho V^2 Sb}\right)$

$C_Y$ lateral-force coefficient $\left(\frac{Y}{\frac{1}{2}\rho V^2 S}\right)$

$C_{D_0}$ profile drag coefficient $\left(\frac{\text{Profile drag}}{\frac{1}{2}\rho V^2 S}\right)$

$v_N$ induced surface velocity normal to wing leading edge

$s$ perpendicular distance of point $(x, y)$ from wing leading edge

$x_{cg}$ distance of center of gravity forward of $\frac{2}{3}c$

Subscripts:

$R$ right edge

$L$ left edge

When $x$, $y$, $z$, or $t$ are used as subscripts, the respective partial derivative is indicated. For example,

$$\phi_x=\frac{\partial\phi}{\partial x}$$

$$\phi_{xt}=\frac{\partial^2\phi}{\partial x\partial t}$$

Whenever $\alpha$, $\dot{\alpha}$, $q$, $p$, $\beta$, and $r$ are used as subscripts, a nondimensional derivative is indicated and this derivative is the slope through zero. For example,

$$C_{m_{\dot{\alpha}}}=\left[\frac{\partial C_m}{\partial\left(\frac{\dot{\alpha}\bar{c}}{2V}\right)}\right]_{\dot{\alpha}\to 0}$$

$$C_{m_q}=\left[\frac{\partial C_m}{\partial\left(\frac{q\bar{c}}{2V}\right)}\right]_{q\to 0}$$

$$C_{l_p}=\left[\frac{\partial C_l}{\partial\left(\frac{pb}{2V}\right)}\right]_{p\to 0}$$

$$C_{l_\beta}=\left[\frac{\partial C_l}{\partial\beta}\right]_{\beta\to 0}$$

$$C_{l_r}=\left[\frac{\partial C_l}{\partial\left(\frac{rb}{2V}\right)}\right]_{r\to 0}$$

A dot above a symbol denotes differentiation with respect to time. All angles are measured in radians.

## ANALYSIS

### SCOPE

The stability derivatives of triangular wings at supersonic speed that have been treated theoretically herein or elsewhere are listed in table I, together with the expressions that have been found for them. All the derivations make use of body axes. The derivations that follow give the values with reference to the principal body axes of figure 2 with origin at the aerodynamic center $\left(\frac{2}{3}c, 0,0\right)$. Conversion has been made to the system of stability axes shown in figure 3 with origin a distance $x_{cg}$ ahead of the $\frac{2}{3}c$ point. Table I comprises parallel columns which present formulas relative to both systems. The expressions are limited to Mach numbers for which the triangle is contained within the Mach cone from its vertex.

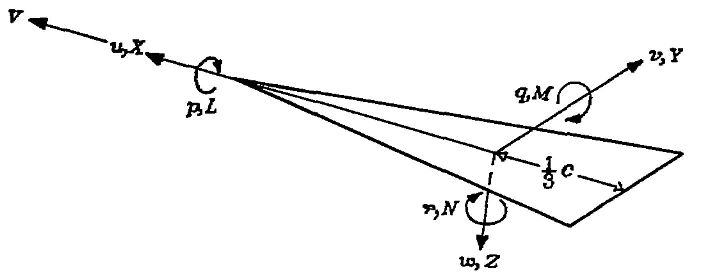


FIGURE 2.—Velocities, forces, and moments relative to principal axes with origin at $\frac{2}{3}c$.

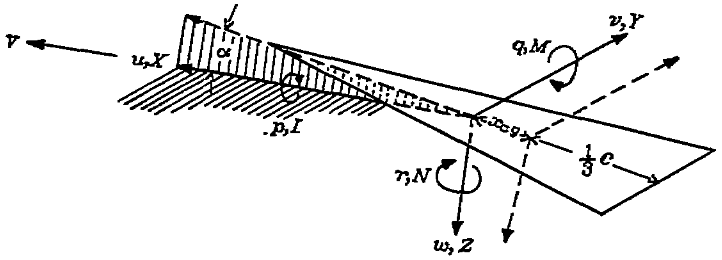


FIGURE 3.—Velocities, forces, and moments relative to stability axes with origin at $\frac{2}{3}c-x_{cg}$. Principal axes of figure 2 dashed in for comparison.

### DERIVATIVE $C_{L_\alpha}$

The pressure distribution on a thin triangular wing at an angle of attack in a supersonic stream has been obtained in references 2 to 4 by the linearized theory without restriction on the vertex angle of the triangle. The approximation originally given for the slender (low-aspect-ratio) triangle (reference 7) and used as the basis for reference 1 is found to apply to the general case upon division by a constant (an elliptic integral) that depends on the ratio of the semivertex angle to the Mach angle; that is,

$$\frac{\Delta P}{\frac{1}{2}\rho V^2}=\frac{4aC\alpha}{E'(BC)\sqrt{a^2-y^2}} \tag{1}$$

where $E'(BC)$ is the complete elliptic integral of the second kind with modulus

$$k=\sqrt{1-B^2C^2}$$
$$=\sqrt{1-(M^2-1)C^2}$$

Thus, the lift-curve slope for the more general case is the value given by references 7 and 1 divided by $E'(BC)$:

$$C_{L_\alpha}=\frac{\pi A}{2E'(BC)}$$
$$=\frac{\pi}{2}AE''(BC) \tag{2}$$

The surface potential given in equation (3) of reference 1 is likewise extended to include nonslender triangles at supersonic speeds upon division by $E'(BC)$. The revised potential is

$$(\phi)_{\pm z=0}=\pm\frac{V\alpha a\sin\eta}{E'(BC)}$$
$$=\pm\frac{V\alpha\sqrt{a^2-y^2}}{E'(BC)} \tag{3}$$

The elliptic integral $E'(BC)$ depends only on the parameter $BC=\frac{\tan\epsilon}{\tan\mu}$ (ratio of the tangent of the semivertex angle of the triangular wing to the tangent of the Mach angle) and is therefore a constant for a given wing at a given speed.

### DERIVATIVES $C_{m_q}$, $C_{L_q}$, AND $C_{l_p}$

The derivatives $C_{m_q}$, $C_{L_q}$, and $C_{l_p}$ are derived in reference 5. With respect to the axes of figure 2

$$C_{m_q}=-\frac{3\pi A}{16}G(BC) \tag{4}$$

$$C_{L_q}=\frac{\pi A}{2}H(BC) \tag{5}$$

$$C_{l_p}=-\frac{\pi A}{32}I(BC) \tag{6}$$

where

$$G(BC)=\frac{1-B^2C^2}{(1-2B^2C^2)E'(BC)+B^2C^2F'(BC)} \tag{7}$$

$$H(BC)=3G(BC)-2E''(BC) \tag{8}$$

$$I(BC)=\frac{2(1-B^2C^2)}{(2-B^2C^2)E'(BC)-B^2C^2F'(BC)} \tag{9}$$

and $F'(BC)$ and $E'(BC)$ are the complete elliptic integrals of the first and second kinds, respectively, with modulus $k=\sqrt{1-B^2C^2}$.

### DERIVATIVES $C_{L_{\dot\alpha}}$ AND $C_{m_{\dot\alpha}}$

The derivation of $C_{L_{\dot\alpha}}$ and $C_{m_{\dot\alpha}}$ in reference 1 is based on the assumption that the steady-state surface potential is not altered in the first order by a small normal acceleration. This assumption is true for the narrow triangles treated in the earlier paper, but it fails for the general triangles treated in the present paper. For this more general case the linearized potential equation for unsteady motion,

$$B^2\phi_{xx}-\phi_{yy}-\phi_{zz}+\frac{2V}{a^2}\phi_{xt}+\frac{1}{a^2}\phi_{tt}=0 \tag{10}$$

must be solved, subject to the boundary condition on the wing, that is, for $z=0$

$$\frac{\partial\phi}{\partial z}=-\dot\alpha Vt \tag{11}$$

In an unpublished paper, Mr. Clifford S. Gardner has, in effect, shown that a suitable solution is

$$\frac{\phi}{\dot\alpha}=\frac{M^2}{B^2}\psi+\left(t-\frac{M^2x}{VB^2}\right)\chi \tag{12}$$

where $\psi$ is the steady-state potential corresponding to a unit pitching velocity about the $y$-axis and $\chi$ is the steady-state potential corresponding to unit angle of attack. That equation (12) is a solution can be verified by direct substitution into equations (10) and (11). *Thus, Gardner has shown that the time-dependent potential for an angle of attack $\dot\alpha t$ may be compounded of two time-free or steady-state potentials, one for a constant angle of attack and the other for steady pitching.*

The lift distribution at time $t=0$ for the angle of attack $\dot{\alpha}t$ is obtained from the surface potential by

$$\begin{aligned}\Delta P&=2\rho(V\phi_x+\phi_t)_{t=0}\\&=2\rho V\dot{\alpha}\left(\frac{M^2}{B^2}\psi_x-\frac{M^2x}{VB^2}\chi_x-\frac{\chi}{VB^2}\right)\\&=\frac{\dot{\alpha}}{B^2}\left[M^2(\Delta P)_{q=1}-\frac{M^2x}{V}(\Delta P)_{\alpha=1}-2\rho\chi\right]\end{aligned}\tag{13}$$

where

$(\Delta P)_{q=1}$ lift distribution for unit pitching velocity about $y$-axis

$(\Delta P)_{\alpha=1}$ lift distribution for unit angle of attack

The choice of time $t=0$ eliminates the lift due to angle of attack and leaves only the increment due to time rate of change of angle of attack.

Integration to obtain the lift and moment and reduction to coefficient form yields

$$C_{L_{\dot{\alpha}}}=\frac{M^2}{B^2}C_{L_q}+\frac{2M^2}{B^2}C_{m_\alpha}-\frac{8}{B^2S\bar{c}}\int\int\frac{\chi}{V}dS\tag{14}$$

$$C_{m_{\dot{\alpha}}}=\frac{M^2}{B^2}C_{m_q}+\frac{2M^2}{B^2S\bar{c}^2}\int\int x^2\left(\frac{\Delta P}{\frac{1}{2}\rho V^2}\right)_{\alpha=1}dS+\frac{8}{B^2S\bar{c}^2}\int\int x\left(\frac{\chi}{V}\right)dS\tag{15}$$

where the integrations are carried over the wing plan form.

For the triangular wing with $y$-axis taken through the aerodynamic center, $\frac{2}{3}c$ from the apex, the derivative $C_{m_\alpha}$ is zero. The derivatives $C_{m_q}$ and $C_{L_q}$ for this case are evaluated in equations (4) and (5), respectively. The potential $\chi$ is obtained by setting $\alpha=1$ in equation (3), and the pressure coefficient $\left(\frac{\Delta P}{\frac{1}{2}\rho V^2}\right)_{\alpha=1}$ is obtained by setting $\alpha=1$ and $a=C\left(\frac{2}{3}c+x\right)$ in equation (1). Substitution, integration, and simplification yields the results

$$C_{L_{\dot{\alpha}}}=-\frac{\pi A}{2}\frac{E''(BC)-M^2H(BC)}{M^2-1}\tag{16}$$

$$C_{m_{\dot{\alpha}}}=\frac{\pi A}{16}\frac{E''(BC)-M^2H(BC)}{M^2-1}\tag{17}$$

### DERIVATIVE $C_{l_\beta}$

The pressure distribution over a thin triangular wing in yaw (sideslip) at an angle of attack at supersonic speed has been obtained in reference 6 and unpublished work. If the angle of yaw is assumed to be small $\left(\beta\ll\frac{1}{M}\right)$, the rolling-moment coefficient can be expressed in the approximate form

$$C_l\approx-\frac{\pi\alpha\beta}{3}E''(BC)$$

Thus, the derivative with respect to $\beta$ is

$$C_{l_\beta}=-\frac{\pi\alpha}{3}E''(BC)\tag{18}$$

An alternative derivation based on the surface potential, equation (3), for the unyawed wing will be given because the method provides the starting point for a derivation of $C_{l_r}$, $C_{Y_\beta}$, $C_{n_\beta}$, $C_{Y_r}$, and $C_{n_r}$.

The potential for the disturbance velocity may be expressed relative to axes alined with the stream (wind axes) or with respect to axes that yaw with the body (body axes). For small angles of yaw $\left(\beta\ll\frac{1}{M}\right)$, the linearized equation for the potential has the same form relative to either system of axes. The potential is determined by the normal velocity of points of the surface and by the orientation of the surface; for negligible thickness, this normal velocity is just $\alpha V$ for all angles of yaw. The potential expressed relative to wind axes thus varies as the wing yaws relative to these axes. The potential expressed relative to body axes is constant for small yaw because the orientation of the wing relative to the axes does not change.

For wind axes, Bernoulli's law has the form

$$\Delta P=2\rho V\frac{\partial\phi}{\partial x}$$

and the change in the pressure distribution with yaw results from the change in the potential function with yaw. For body axes with small yaw, Bernoulli's law has the approximate form

$$\Delta P=2\rho V\left(\frac{\partial\phi}{\partial x}-\beta\frac{\partial\phi}{\partial y}\right)\tag{19}$$

and the change in pressure distribution with yaw results from the term $-\beta\frac{\partial\phi}{\partial y}$ since $\phi$ does not change.

In reference 1 in the section entitled "Derivative $C_{l_\beta}$," the derivation employs body axes and equation (19) of the present paper. The surface potential used (equation (3) of reference 1) is the approximation for narrow vertex angle. Equation (3) herein for a general vertex angle may be used instead. Equation (3) herein differs only in the factor $1/E'(BC)$, whence the earlier expression for $C_{l_\beta}$ (equation (19), reference 1, with $\Gamma=0°$) acquires this factor to agree with equation (18).

### DERIVATIVE $C_{l_r}$

The foregoing discussion of the triangular wing in yaw (sideslip) may be extended to provide a preliminary treatment of the case of a small angular velocity of yaw $r$. The corresponding extension for narrow vertex angle is made in reference 1. The treatment is generalized to an arbitrary vertex angle for supersonic speeds, as before, by using equation (3) herein for the surface potential. Two changes then appear in the pressure equation, equation (20), of reference 1. The right-hand side is divided by $E'(BC)$, and the term $aC=xC^2$ must be retained since $C^2$ is no longer small compared with unity ($C$=Tangent of semivertex angle). With these changes, the derivation leads to

$$C_{l_r}=\pi\alpha\left(\frac{1}{9A}+\frac{A}{16}\right)E''(BC)\tag{20}$$

In the derivation of equation (20), the spanwise variation in local Mach number caused by yawing is not taken into account although the variation in forward speed is taken into account. The surface potential that is used, equation (3), satisfies the linearized equation for a flow of uniform Mach number. This potential is inadequate to describe the compressibility effects associated with a spanwise variation of Mach number.

Thus, consider a high-aspect-ratio rectangular wing with tips cut off along the Mach lines. In straight flight the Ackeret theory can be applied. The pressure difference is given by

$$\Delta P=\alpha\frac{2\rho M^2\ (\text{Speed of sound})^2}{\sqrt{M^2-1}} \tag{21}$$

In yawing flight the forward velocity varies linearly along the span. If the rate of yaw is made sufficiently low, the variation from wing tip to wing tip can be made so small that the flow is still nearly two-dimensional at any point. Thus the Ackeret theory is still applicable if the local Mach number is used at each spanwise station.

The variation in pressure with local Mach number can be obtained from equation (21). As the Mach number is increased, the pressure decreases from infinity at $M=1$ to a minimum at $M=1.4$ and then increases again. Thus below Mach number 1.4 the faster moving sections of the yawing wing have the lesser lift. This result is contrary to subsonic behavior and to that which would be predicted if the spanwise variation of Mach number were neglected. Thus the spanwise variation of the compressibility effect causes a reversal of the sign of the rolling moment due to yawing for rectangular wings at Mach numbers between 1 and 1.4, and at $M=1.4$ the moment is zero. (This result refers to yawing in a system of stability axes, fig. 3. For body axes, fig. 2, the effect is similar but the reversal extends to $M=\infty$.)

A yawing triangular wing may be expected likewise to show an effect of the spanwise variation in Mach number. If the triangle is contained within the Mach cone from its vertex (the only case considered in this report), however, the effect should be very much less than for the rectangular wing. In particular, where the predicted effect for the rectangular wing is a reversal of the sign of the rolling moment, the effect for the triangular wing is expected to be merely a change in the magnitude. A reversal in sign is not expected until the edges of the triangle protrude from the Mach cone. This behavior is inferred from the fact that the analyses of references 2 to 7 show many subsonic characteristics for triangles within the Mach cone and a marked change in characteristics for triangles with side edges outside the Mach cone.

### DERIVATIVES $C_{Y_p}$ AND $C_{n_p}$

Extensive changes are necessary to generalize the treatment of $C_{Y_p}$ and $C_{n_p}$ in reference 1 to arbitrary vertex angles for supersonic speeds; therefore, the revised derivation is given in detail.

The derivatives $C_{Y_p}$ and $C_{n_p}$ relative to body axes for a very thin triangular wing without dihedral arise entirely from suction on the wing side edges. Consider a condition for which the induced velocity normal to the edge is of the form

$$v_N=\pm\frac{K}{\sqrt{s}} \tag{22}$$

in the immediate neighborhood of the edge, where $s$ is the perpendicular distance from the edge and $K$ is a constant. Reference 3 points out that for such a flow there is a suction force per unit length of edge,

$$f=\pi\rho K^2\sqrt{1-M'^2} \tag{23}$$

so long as the triangular wing does not protrude from the Mach cone from its vertex. In equation (23), $M'$ is the Mach number of the component of the stream flow normal to the leading edge. The radical $\sqrt{1-M'^2}$ is the Prandtl-Glauert compressibility factor for the normal component of flow. Equation (23) is limited to real values of the radical by the condition expressed for the Mach cone.

For the delta wing in rolling motion the induced velocity component $u$ has been obtained in reference 5 as

$$u_1=\pm\frac{pyC^2}{2\sqrt{C^2-\left(\frac{y}{x}\right)^2}}I(BC)$$

Angle of attack gives the additional contribution (reference 2)

$$u_2=\pm\frac{\alpha VC^2}{E'(BC)\sqrt{C^2-\left(\frac{y}{x}\right)^2}}$$

The total induced velocity on the upper surface is thus the sum of $u_1$ and $u_2$ with the plus sign

$$u=\frac{C^2}{\sqrt{C^2-\left(\frac{y}{x}\right)^2}}\left[\frac{\alpha V}{E'(BC)}+\frac{py}{2}I(BC)\right]$$

Very near the side edge this velocity is approximately

$$u=\frac{C^{3/2}}{\sqrt{2\left(C-\left|\frac{y}{x}\right|\right)}}\left[\frac{\alpha V}{E'(BC)}\pm\frac{pCx}{2}I(BC)\right]$$

where the plus sign refers to the right edge and the minus sign to the left edge.

If a similar calculation is made for $v=\frac{\partial\phi}{\partial y}$, it is found that as the side edge is approached the resultant induced velocity $\sqrt{u^2+v^2}$ becomes normal to the edge. Thus the normal velocity near the edge is

$$v_N=\frac{\sqrt{1+C^2}}{C}u$$

The perpendicular distance of point $(x, y)$ from the side edge is

$$s=\frac{x\left(C-\left|\frac{y}{x}\right|\right)}{\sqrt{1+C^2}}$$

The resultant induced velocity very near the edge may therefore be expressed approximately as

$$v_N=\pm\left[\frac{\alpha V}{E'(BC)}\pm\frac{I(BC)pCx}{2}\right](1+C^2)^{1/4}\left(\frac{Cx}{2s}\right)^{1/2}$$

which is of the form of equation (22). The suction force per unit length of edge is from equation (23) thus

$$f=\frac{\pi}{2}\rho Cx\left\{\frac{\alpha^2V^2}{[E'(BC)]^2}+\frac{[I(BC)]^2p^2C^2x^2}{4}\pm\frac{I(BC)\alpha VpCx}{E'(BC)}\right\}\sqrt{(1+C^2)(1-M'^2)} \tag{24}$$

where the plus sign refers to the right edge and the minus sign refers to the left edge. The factor $\sqrt{(1+C^2)(1-M'^2)}$ can be reduced to $\sqrt{1-B^2C^2}$, where $B^2=M^2-1$.

The lateral component of this suction force is given by

$$Y=\int_0^c (f_R-f_L)dx$$
$$=\frac{\pi}{3}\rho C^2c^3\alpha Vp\frac{I(BC)\sqrt{1-B^2C^2}}{E'(BC)}$$

The lateral-force coefficient is formed by division by $\frac{1}{2}\rho V^2S$, and the derivative with respect to $pb/2V$ is the stability derivative $C_{Y_p}$. It is

$$C_{Y_p}=\frac{2\pi\alpha}{3}\frac{I(BC)\sqrt{1-B^2C^2}}{E'(BC)} \tag{25}$$

The yawing moment of the leading-edge suction about the vertex of the triangle is

$$N_0=-\int_{x=0}^{c}(f_R-f_L)\,x\sqrt{1+C^2}\;d(x\sqrt{1+C^2})$$
$$=-\frac{\pi}{4}\rho C^2c^4\alpha Vp(1+C^2)\frac{I(BC)\sqrt{1-B^2C^2}}{E'(BC)}$$

The moment about the reference point $\left(\frac{2}{3}c,0,0\right)$ is

$$N=N_0+\frac{2}{3}cY$$
$$=-\frac{\pi}{36}\rho C^2c^4\alpha Vp(1+9C^2)\frac{I(BC)\sqrt{1-B^2C^2}}{E'(BC)}$$

The yawing-moment coefficient is formed by division by $\frac{1}{2}\rho V^2Sb$, and the derivative with respect to $pb/2V$ is the stability derivative $C_{n_p}$. It is

$$C_{n_p}=-\pi\alpha\left(\frac{1}{9A}+\frac{A}{16}\right)\frac{I(BC)\sqrt{1-B^2C^2}}{E'(BC)} \tag{26}$$

DERIVATIVES $C_{Y_\beta}$, $C_{n_\beta}$, $C_{Y_r}$, AND $C_{n_r}$

According to the discussion on $C_{l_\beta}$, a small angle of yaw or sideslip $\left(\beta\ll\frac{1}{M}\right)$ does not alter the surface potential (to the first order in $\beta$) expressed relative to body axes. Thus, the initially symmetric distribution of leading-edge velocity persists in sideslip. The symmetry of the leading-edge suction is, however, upset by the sideslip because of a compressibility effect. The quantitative evaluation of the change proceeds as follows:

Equation (23) expresses the suction per unit length of edge in the form

$$f=\pi\rho K^2\sqrt{1-M'^2}$$

For infinitesimal sideslip the constant $K$, related to the edge velocity, is unchanged, but $M'$, the component Mach number perpendicular to the edge, is altered: $M'$ increases on the right edge and decreases on the left edge. Because of the change of $M'$ with sideslip angle $\beta$ the edge suction may be written, for small values of $\beta$,

$$f=f_{\beta=0}+\beta\left(\frac{\partial f}{\partial\beta}\right)_{\beta=0} \tag{27}$$

By differentiation of equation (23), with $K$ constant and $M'=M\sin(\epsilon\pm\beta)$, there results

$$f=f_{\beta=0}\mp\beta f_{\beta=0}\left(\frac{M'^2\cot\epsilon}{1-M'^2}\right)_{\beta=0} \tag{28}$$

where the upper sign refers to the right edge and the lower sign to the left edge.

The quantity $f_{\beta=0}$ is obtained by setting $p=0$ in equation (24):

$$f_{\beta=0}=\frac{\pi\rho Cx\alpha^2V^2\sqrt{1-B^2C^2}}{2[E'(BC)]^2} \tag{29}$$

Substitution of equation (29) in the last term of equation (28) and simplification, with $\tan\epsilon=C$, yields

$$f=f_{\beta=0}\mp\beta\frac{\pi\rho V^2\alpha^2xC^2M^2}{2[E'(BC)]^2\sqrt{1-B^2C^2}} \tag{30}$$

Equation (30) gives the suction per unit length of edge for a triangular wing with an angle of sideslip $\beta$.

For the case of a small angular velocity of yaw $r$, the edge suction may be approximated by

$$f=f_{r=0}+r\left(\frac{\partial f}{\partial r}\right)_{r=0}$$

where $f_{r=0}$ is the same as $f_{\beta=0}$ and is given by equation (29). If the center of rotation is at the reference point $\left(\frac{2}{3}c,0,0\right)$, the component Mach number normal to the edges is

$$M'=M\left[\sin\epsilon\pm\frac{r}{V}\left(\frac{2}{3}c\cos\epsilon-x\sec\epsilon\right)\right]$$

This value of $M'$ is to be incorporated in equation (23) for $f$ before the indicated differentiation $\frac{\partial f}{\partial r}$ can be carried out. The final result is

$$f=f_{\beta=0}\mp r\,\frac{\left(\frac{2}{3}c-x\sec^2\epsilon\right)\pi\rho V\alpha^2xC^2M^2}{2\,[E'(BC)]^2\sqrt{1-B^2C^2}} \tag{31}$$

The difference between the suction forces on the right and left edges, as determined from equations (30) and (31), has been integrated to yield values of side force and yawing moment. The procedures, and the subsequent reduction to coefficient form, are similar to those leading to equation (25) for $C_{Y_p}$ and to equation (26) for $C_{n_p}$. The results are

$$\left.\begin{aligned}
C_{Y_\beta}&=-\frac{\pi}{4}\alpha^2AM^2Q(BC)\\
C_{n_\beta}&=\frac{\pi}{48}\alpha^2A^2M^2Q(BC)\\
C_{Y_r}&=\frac{\pi}{24}\alpha^2A^2M^2Q(BC)\\
C_{n_r}&=-\frac{\pi\alpha^2M^2}{9}\left(\frac{1}{A}+\frac{A}{8}+\frac{9A^3}{256}\right)Q(BC)
\end{aligned}\right\} \tag{32}$$

where

$$Q(BC)\equiv\frac{[E''(BC)]^2}{\sqrt{1-B^2C^2}}$$

The analysis thus far has been based on potential-flow theory. A little consideration will show that the direct viscous effect—that is, the skin-friction drag—will have a negligible effect on all the stability derivatives studied herein except $C_{n_r}$. To this derivative the skin friction will add an increment

$$\Delta C_{n_r}=-C_{D_0}\left(\frac{1}{6}+\frac{4}{9A^2}\right)$$

as determined in reference 1.

## RESULTS AND DISCUSSION

The formulas that have been obtained for the various stability derivatives are collected in table I. Derivatives obtained elsewhere are included for completeness, and the source is indicated in each instance. Expressions are given for two systems of coordinate axes. In the first column are shown the derivatives relative to the principal body axes of figure 2 with origin a distance $\frac{2}{3}c$ from the vertex of the triangle. In the second column are shown the results relative to stability axes with origin a distance $x_{cg}$ ahead of the $\frac{2}{3}c$ point. The relationship between the two systems of axes is shown in figure 3. Equations for transforming from body axes to stability axes are given in reference 8; the shift in origin results in additional terms.

In the transformation of the present results from principal body axes to stability axes terms of order $A^2/16$ and the more important terms of order $\alpha^2$ are retained (see footnote, table I), whereas in reference 1 such terms are dropped as a consequence of the narrow vertex-angle approximation.

These results for an arbitrary vertex angle may be compared with the asymptotic values for the case of vertex angle approaching zero given in reference 1. The present results for principal axes are found to differ from the asymptotic values (except for small terms in $A^2$ and $\alpha^2$) only in the acquisition of certain factors which in general are functions of $BC$. Thus $C_{L_\alpha}$, $C_{l_\beta}$, and $C_{l_r}$ of reference 1 are multiplied by $E''(BC)$; $C_{m_q}$ is multiplied by $G(BC)$; $C_{L_q}$ is multiplied by $H(BC)$; $C_{l_p}$ is multiplied by $I(BC)$; $C_{n_p}$ and $C_{Y_p}$ are multiplied by

$$\frac{I(BC)\sqrt{1-B^2C^2}}{E'(BC)}\equiv J(BC)$$

and $C_{L_{\dot\alpha}}$ and $C_{m_{\dot\alpha}}$ are multiplied by

$$\frac{M^2H(BC)-E''(BC)}{M^2-1}$$

The parameter $BC=\frac{\tan\epsilon}{\tan\mu}$ is the ratio of tangent of the semivertex angle of the triangle to the tangent of the Mach angle; $BC$ approaches zero, therefore, as the vertex angle approaches zero. The several functions $E''(BC)$, . . . $J(BC)$ all approach unity as $BC$ approaches zero, and thus the derivatives obtained herein approach the asymptotic values of reference 1 as the vertex angle goes to zero.

The variation of the stability derivatives with Mach number (except $C_{L_{\dot\alpha}}$ and $C_{m_{\dot\alpha}}$) is contained entirely in the factors $E''(BC)$, . . . $J(BC)$ and an additional factor $Q(BC)\equiv\frac{[E''(BC)]^2}{\sqrt{1-B^2C^2}}$. The six factors are plotted against $BC=\frac{\tan\epsilon}{\tan\mu}$, the ratio of the tangent of the semivertex angle to the tangent of the Mach angle, in figure 4.

The derivatives apply to a wing of triangular plan form and zero thickness. The calculations are based on the assumption of potential flow with small disturbances, except in the case of the derivative $C_{n_r}$, in which skin friction is considered. The predicted infinite negative pressure acting on an edge of zero thickness to yield a finite suction force is, of course, a mathematical idealization. (The local violation of the assumption of small disturbances is not serious.) Subsonic experience indicates that with a suitably rounded edge a considerable leading-edge suction force may be realized in practice, with the theoretical value an upper limit. On the other hand, a sharp leading edge is known to cause loss of the leading-edge suction. The requirements of extreme thinness and a rounded leading edge (that is, appreciable radius of curvature) are evidently in conflict. Thus, the degree of applicability of the yawing-moment and lateral-force derivatives to actual triangular wings is uncertain. A

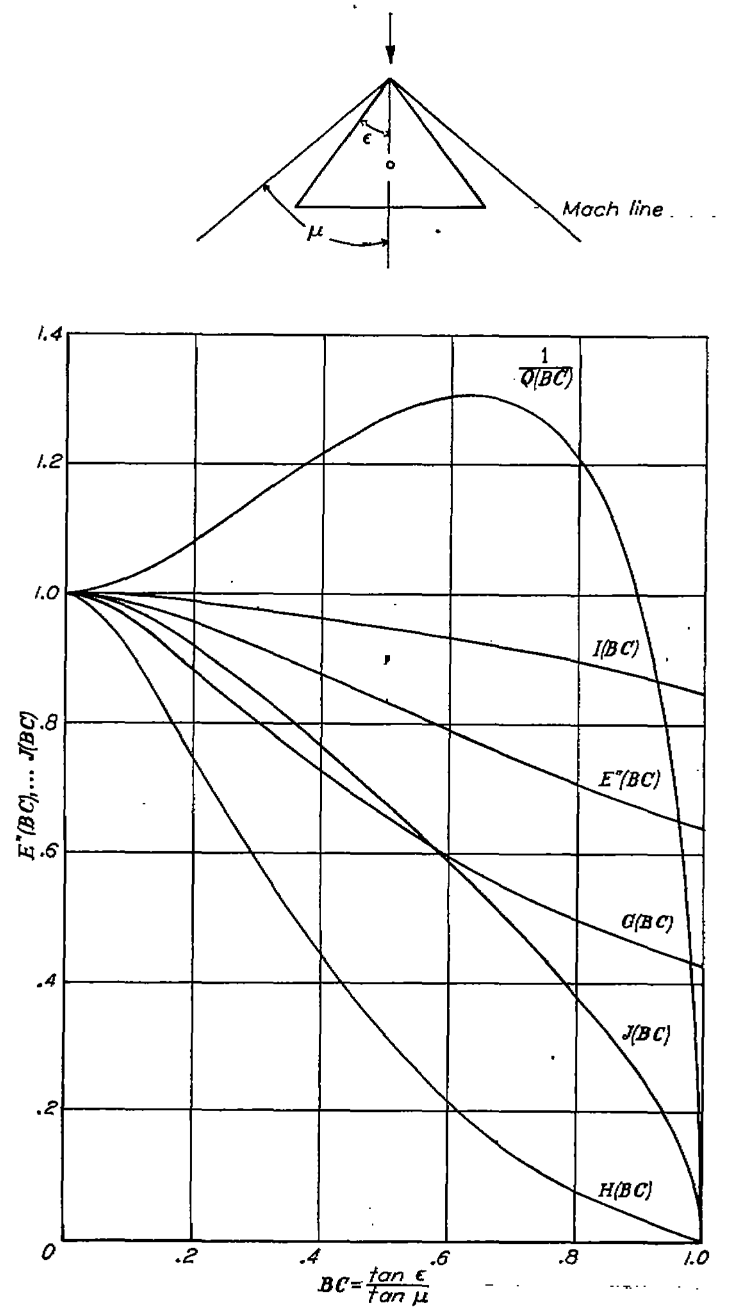


FIGURE 4.—Elliptic integral factors of the stability derivatives that determine their variation with Mach number. (See table I.)

further limitation on validity, already elaborated on in the section on $C_{l_r}$, exists also for the derivatives with respect to yawing velocity. The analysis neglects the spanwise variation in Mach number caused by the yawing (but not the spanwise variation in velocity). The result is an error in the magnitude of the yawing derivatives that is expected to vary from zero for $BC \rightarrow 0$ to an important amount for $BC \rightarrow 1$.

The potential $\phi$ satisfies the linearized equation of motion for the steady state but not the more general linearized equation for unsteady motion except for the case of normal acceleration ($\dot{\alpha}$). This circumstance implies that the present expressions for the stability derivatives are suitable only for steady motions, motions with small accelerations, or sinuous motions of low frequency. This limitation is accepted in all stability work and may become serious only in cases of high-frequency oscillations such as flutter.

LANGLEY MEMORIAL AERONAUTICAL LABORATORY,
NATIONAL ADVISORY COMMITTEE FOR AERONAUTICS,
LANGLEY FIELD, VA., *November 6, 1947.*

## REFERENCES


1. Ribner, Herbert S.: The Stability Derivatives of Low-Aspect-Ratio Triangular Wings at Subsonic and Supersonic Speeds. NACA TN No. 1423, 1947.
2. Stewart, H. J.: The Lift of a Delta Wing at Supersonic Speeds. Quarterly Appl. Math., vol. IV, no. 3, Oct. 1946, pp. 246–254.
3. Brown, Clinton E.: Theoretical Lift and Drag of Thin Triangular Wings at Supersonic Speeds. NACA Rep. No. 839, 1946.
4. Gurevich, M. I.: Lift Force of An Arrow-Shaped Wing. Appl. Math. and Mech. (Moscow), vol. X, no. 4, 1946, pp. 513–520.
5. Brown, Clinton E., and Adams, Mac C.: Damping in Pitch and Roll of Triangular Wings at Supersonic Speeds. NACA Rep. No. 892, 1948.
6. Heaslet, Max. A., Lomax, Harvard, and Jones, Arthur L.: Volterra's Solution of the Wave Equation as Applied to Three-Dimensional Supersonic Airfoil Problems. NACA TN No. 1412, 1947.
7. Jones, Robert T.: Properties of Low-Aspect-Ratio Pointed Wings at Speeds below and above the Speed of Sound. NACA Rep. No. 835, 1946.
8. Glauert, H.: A Non-Dimensional Form of the Stability Equations of an Aeroplane. R. & M. No. 1093, British A.R.C., 1927, p. 10.

TABLE I.—STABILITY DERIVATIVES OF THIN TRIANGULAR WINGS AT SUPERSONIC SPEEDS

| Derivative | Source | Principal body axes $\left(\text{origin at } \frac{2}{3}c\right)$ | Stability axes[1] $\left(\text{origin at distance } x_{cg} \text{ ahead of } \frac{2}{3}c \text{ point}\right)$ |
|---|---|---|---|
| $C_{L_\alpha}$ | References 2 to 4 | $\frac{\pi A}{2}E''(BC)$ | $\frac{\pi A}{2}E''(BC)$ |
| $C_{L_{\dot{\alpha}}}$ | Present report | $-\frac{\pi A}{2}\frac{E''(BC)-M^2H(BC)}{M^2-1}$ | $-\frac{\pi A}{2}\frac{E''(BC)-M^2H(BC)}{M^2-1}$ |
| $C_{L_q}$ | Reference 5 | $\frac{\pi A}{2}H(BC)$ | $\frac{\pi A}{2}H(BC)+\pi A\frac{x_{cg}}{c}E''(BC)$ |
| $C_{m_\alpha}$ | References 2 to 4 | 0 | $-\frac{\pi A}{2}\frac{x_{cg}}{c}E''(BC)$ |
| $C_{m_{\dot{\alpha}}}$ | Present report | $\frac{\pi A}{16}\frac{E''(BC)-M^2H(BC)}{M^2-1}$ | $\frac{\pi A}{16}\left(1+8\frac{x_{cg}}{c}\right)\frac{E''(BC)-M^2H(BC)}{M^2-1}$ |
| $C_{m_q}$ | Reference 5 | $-\frac{3\pi A}{16}G(BC)$ | $-\frac{3\pi A}{16}G(BC)-\frac{\pi A}{2}\frac{x_{cg}}{c}H(BC)-\pi A\frac{x_{cg}^2}{c^2}E''(BC)$ |
| $C_{l_\beta}$ | Reference 6 | $-\frac{\pi\alpha}{3}E''(BC)$ | $-\frac{\pi\alpha}{3}E''(BC)$ |
| $C_{l_p}$ | Reference 5 | $-\frac{\pi A}{32}I(BC)$ | $-\frac{\pi A}{32}I(BC)+\frac{\pi\alpha^2}{9A}\left(1+8\frac{x_{cg}}{c}\right)[E''(BC)-J(BC)]$ |
| $C_{l_r}$ | Present report | $\pi\alpha\left(\frac{1}{9A}+\frac{A}{16}\right)E''(BC)$ | $\pi\alpha\left[\left(\frac{1}{9A}+\frac{A}{16}+\frac{8}{9A}\frac{x_{cg}}{c}\right)E''(BC)+\frac{A}{32}I(BC)\right]-\alpha C_{D_0}\left(\frac{1}{6}+\frac{4}{9A^2}\right)$ |
| $C_{n_\beta}$ | do | $\frac{\pi}{48}\alpha^2A^2M^2Q(BC)$ | $\frac{\pi\alpha^2}{3}\left[E''(BC)+\left(\frac{A^2}{16}+\frac{x_{cg}}{c}\right)M^2Q(BC)\right]$ |
| $C_{n_p}$ | do | $-\pi\alpha\left(\frac{1}{9A}+\frac{A}{16}\right)J(BC)$ | $-\pi\alpha\left[\left(\frac{1}{9A}+\frac{A}{16}+\frac{8}{9A}\frac{x_{cg}}{c}\right)J(BC)-\frac{A}{32}I(BC)\right]-\alpha C_{D_0}\left(\frac{1}{6}+\frac{4}{9A^2}\right)$ |
| $C_{n_r}$ | Term in $C_{D_0}$ derived in reference 1. | $-C_{D_0}\left(\frac{1}{6}+\frac{4}{9A^2}\right)-\frac{\pi\alpha^2M^2}{9}\left(\frac{1}{A}+\frac{A}{8}+\frac{9A^3}{256}\right)Q(BC)$ | $-C_{D_0}\left(\frac{1}{6}+\frac{4}{9A^2}\right)-\pi\alpha^2\left(\frac{1}{9A}+\frac{A}{16}+\frac{8}{9A}\frac{x_{cg}}{c}\right)[E''(BC)-J(BC)]-\pi\alpha^2\frac{A}{32}I(BC)-\frac{\pi\alpha^2M^2}{9}\left(\frac{1}{A}+\frac{A}{8}+\frac{9A^3}{256}+A\frac{x_{cg}}{c}+\frac{8}{A}\frac{x_{cg}^2}{c^2}\right)Q(BC)$ |
| $C_{Y_\beta}$ | Present report | $-\frac{\pi}{4}\alpha^2AM^2Q(BC)$ | $-\frac{\pi}{4}\alpha^2AM^2Q(BC)$ |
| $C_{Y_p}$ | do | $\frac{2\pi\alpha}{3}J(BC)$ | $\frac{2\pi\alpha}{3}J(BC)$ |
| $C_{Y_r}$ | do | $\frac{\pi}{24}\alpha^2A^2M^2Q(BC)$ | $\frac{2\pi\alpha^2}{3}\left[-J(BC)+\left(\frac{A^2}{16}+\frac{x_{cg}}{c}\right)M^2Q(BC)\right]$ |

[1] In the transformation from body axes, terms of order $\alpha^2$ have been neglected in comparison with unity, but terms of order $\alpha^2/A$ have been retained since they may be appreciable for small values of $A$.